On the application of asymptotic reduction methods of slender structures to fluid–structure interaction problems

Carlos E.S. Cesnik*, Rafael Palacios

Department of Aerospace Engineering, University of Michigan, 1320 Beal Avenue, Ann Arbor, Michigan, MI 48109, USA

Abstract

A methodology for the aeroelastic analysis of highly flexible slender structures is presented. The structural model is based on an asymptotic approximation to the displacement field, which separates the problem into a long-scale problem involving geometrically-nonlinear deformations of the reference line and a small-scale problem that captures deformation in the cross section. The combination of them provides a three-dimensional solution to the structural dynamics of flexible vehicles suitable for aeroelastic simulations.

Keywords: Slender structures; Asymptotic methods; Fluid–structure interaction

1. Introduction

A general characteristic of high aspect-ratio-winged vehicles is that they are easily subject to large wing deflections under aerodynamic loads, which yields significant variations of the aircraft geometry during flight. For a meaningful characterization of this situation, aeroelastic analysis on very flexible vehicles should then incorporate geometrically-nonlinear effects in the description of the structural displacement field. Typically, these effects can be associated to the deformation of a reference line in the structure, and the problem is then usually studied using nonlinear beam models. Beam models offer a good representation of the average motions along the reference line, but they also assume that cross sections remain rigid in the coupling with the aerodynamics. Although this assumption works well under smoothly distributed loads, local deformations may affect the characteristics of the flow field in aeroelastic analyses and a more detailed representation of the structure including the small cross-sectional deformations would be desirable. Asymptotic theories offer an effective way of refining the kinematical description of the deformation, as it was done for the analysis of composite beams by Cesnik et al. [1], and later for the general problem of 3-D electroelasticity by Palacios et al. [2]. The presence of a small parameter (the inverse of the wing aspect ratio) allows an asymptotic approximation to the equations of elasticity in the 3-D domain, which are then decomposed into two independent variational problems: cross-sectional (small-scale) and longitudinal (long-scale) analyses. The cross-sectional problem solves the local deformation field for unit value of the long-scale variables. The longitudinal problem solves the average deformation of the reference line under given external loads. Both problems are tightly coupled and together provide the necessary description of the displacement field in the 3-D domain. Furthermore, the longitudinal problem does not need to be restricted to the usual degrees of freedom of beam analysis and can be expanded through a modal expansion in the cross-sectional displacement field. They are measures of non-classical motions, such as plate-like deformations in thin-walled structures, and are defined as *finite-section modes* in [2]. This paper shows an application of this methodology to define the solid side in fluid–structure problems.

* Corresponding author. Tel.: +1 (734) 764 3397; Fax: + 1 (734) 763 0978; E-mail: cesnik@umich.edu

2. Asymptotic reduction of the dynamics of a slender structure

Figure 1 shows the proposed scheme for the aeroelastic analysis of slender structures. An arbitrary reference line is first defined along the dominant dimension of the undeformed structure, with curvilinear coordinate x_1. The pair (x_2, x_3) describes the planar

Computational Fluid and Solid Mechanics 2005
K.J. Bathe (Editor)
Written under government grant (NASA Langley Research Center NAG-1-03038)

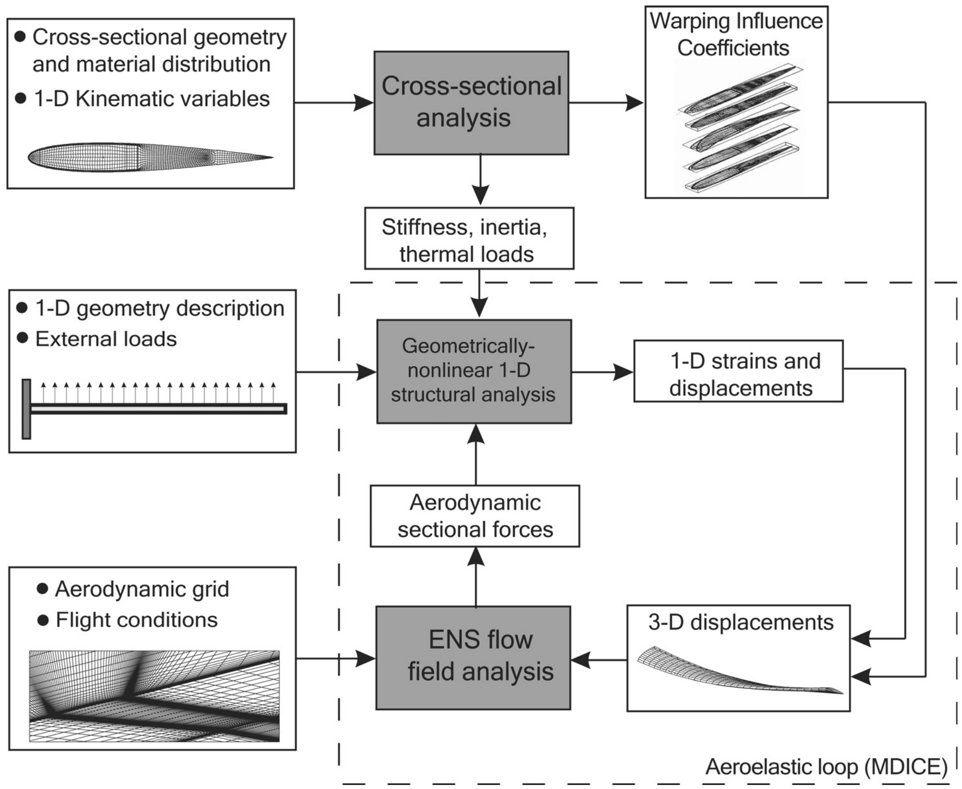

Fig. 1. Scheme for aeroelastic simulations using asymptotic reduction of the structure.

cross sections, which do not need to be normal to the reference line (i.e. oblique sections along aerodynamic airfoils in a swept wing).

2.1. Small-scale problem

The slenderness parameter is now used to approximate the strain energy per unit length as $2\mathrm{U}(x_1) = \int_{CS} \Gamma^T \Sigma dx_2 dx_3$, where Γ and Σ are the vector forms of the local strain and stress tensors, respectively. The domain of integration is the local cross section at x_1. It is assumed that the local elastic problem is linear (small strains and local rotations).

The 1-D representation of the deformation of the reference line is chosen at this point. The baseline are naturally the four intrinsic deformation magnitudes for the elastic curve, i.e. extension, γ_{11}, and three curvatures $\{\kappa_1,\kappa_2,\kappa_3\}$. In addition to them, a set of *finite-section deformation modes* are defined using assumed distributions of displacements in the cross section, $\psi_q(x_2,x_3)$. The vector of their amplitudes, $q(x_1)$, as well as its first derivative, $q'(x_1)$, adds elastic variables to the reduced 1-D model, which is finally defined by $\chi = \{\gamma_{11},\kappa_1,\kappa_2,\kappa_3,q,q'\}$. Without any loss of generality, the local small strain Γ in a cross section can be rewritten in terms of the 1-D measures, χ, and an unknown warping field, $\bar{\mathrm{w}}$, as

$$\Gamma(x_1,x_2,x_3) = \Gamma_\chi \chi(x_1) + \Gamma_w \bar{w}(x_1,x_2,x_3) + \Gamma_{w'} \frac{\partial \bar{w}}{\partial x_1}(x_1,x_2,x_3) \tag{1}$$

where the Γ-operators are linear matrix operators defined in [1]. At this point one can set up the small-scale variational problem as

$$\delta \mathrm{U}(\bar{w};\chi) = 0, \text{for } \chi \text{ prescribed} \tag{2}$$

$\bar{\mathrm{w}}$ is discretized using a finite-element representation in the cross section and is then solved as a function of χ using asymptotic expansions in the small parameter. As a result of this linear optimal problem, one gets a set of warping influence coefficients (*WIC*), defined as $\mathrm{WIC} = \frac{\partial \bar{\mathrm{w}}}{\partial \chi}$, with which the strain energy can be rewritten as a bilinear operator in the 1-D variables, whose coefficient matrix defines the stiffness per unit length:

$$S = \left\{ I \quad WIC^T \right\} \begin{bmatrix} \frac{\partial^2 \mathrm{U}}{\partial \chi^2} & \frac{\partial^2 \mathrm{U}}{\partial \chi \partial \bar{w}} \\ \frac{\partial^2 \mathrm{U}}{\partial \bar{w} \partial \chi} & \frac{\partial^2 \mathrm{U}}{\partial \bar{w}^2} \end{bmatrix} \left\{ \begin{matrix} I \\ WIC \end{matrix} \right\} \tag{3}$$

The mass matrix corresponding to the selected 1-D description of the beam kinematics is obtained by a similar procedure, starting with the kinetic energy per unit length. See [2] for further details.

2.2. Long-scale problem

The dynamics at the reference line are analyzed under the following assumptions:

1. large displacements and global rotations of the reference line;
2. small values of strains and local rotations;
3. small amplitudes of the finite-section modes, q.

A geometrically-exact description the kinematics of the reference line is used. Appropriate differentiation in time and space of the displacement/rotation variables $\{u(t,x_1),\ \theta(t,x_1)\}$ yields the beam velocities $\{V(t,x_1), \Omega(t,x_1)\}$, and strains $\{\gamma(t,x_1),\ \kappa(t,x_1)\}$. The amplitudes of the finite-section modes, $q(t,x_1)$, and their corresponding strain and velocity measures, q' and $\dot{q}$, are then superimposed. The final independent variables in the reduced 1-D problem are

$$z(t,x_1) = (u, \theta, q, \gamma, \kappa, q', V, \Omega, \dot{q}) \tag{4}$$

The kinetic and strain energy per unit length, T and U, and the work per unit length of the external forces, W, can be written in terms of those variables, what defines all magnitudes for the long-scale variational problem. For each continuous subcomponent in the 1-D domain of arclength l, Hamilton's Principle is invoked. This is solved with a spatial finite-element discretization of z, named Z, which yields time-domain nonlinear equations of the form

$$\begin{aligned} &A(Z)\cdot\dot{Z} = F_S(Z,\hat{Z}_{x=0},\hat{Z}_{x=l}) - F_L \\ &BC(\hat{Z}_{x=0}) = 0 \text{ and } BC(\hat{Z}_{x=l}) = 0 \end{aligned} \tag{5}$$

where A is the inertia matrix operator, F_s is the structural vector operator, and F_L is the force vector operator. $\hat{Z}$ contains the boundary values of the state vector Z, and BC are boundary conditions.

2.3. Definition of the fluid–structure interface

All previous results are combined at each time step to recover the actual displacements in the original domain. Let $r(t,x)$ be the instant position vector of a point (x_1,x_2,x_3) in the fluid-structure interface in the undeformed configuration, and let $\xi = (0,x_2,x_3)$ be the position of that point in its corresponding cross section. Its position vector after deformation is

$$\begin{aligned} R = {} & r(t,x_1) + u(t,x_1) + \theta(t,x_1)\times\xi(x_2,x_3) + \psi_q(x_1,x_2,x_3) \\ & q(t,x_1) + WIC(x_1,x_2,x_3)\chi(t,x_1) \end{aligned} \tag{6}$$

At each time step, this structural displacement field is passed to the mesh deformation algorithm that updates the fluid domain discretization before the next iteration in the fluid-dynamics equations. Finally, integration along the contour of each cross section of the aerodynamic forces per unit surface, f, give the contributions per unit length to the force vector operator F_L in Eq. (5), i.e.

$$F = \oint f ds;\ M = \oint \xi\times f ds;\ F_q = \oint \psi_q\cdot f ds \tag{7}$$

3. Application to a modified AGARD445.6 wing

The present structural formulation is coupled with the Euler equations in ENS3DAE [3] using MDICE [4] and is applied to the AGARD445.6 wing [5]. Although this is clearly not a slender configuration, the availability of CFD grids and a good number of benchmark results made this wing a good test case for the implementation of the proposed formulation. The cantilever wing has quarter-chord sweep angle of 45°, root chord $c_r = 0.5588\,\text{m}$, semispan $b = 0.762\,\text{m}$, and taper ratio 0.66. A modified (weakened) structural model is defined for the purposes of the present analysis, based on a constant-thickness isotropic material for the skin and the spar. The parameters in the analysis are skin and spar thickness, t, free-stream Mach number, M_∞, and root angle of attack, α. Flight is set at sea-level and the location of the spar at 40% of the local chord.

Generation of the cross-sectional and longitudinal finite-element models is automated for easy parameterization of the geometric configuration and material distribution. In order to consider the variation of properties along the span, properties are computed at the oblique sections at wing root and tip and interpolated in the interior points. Warping information is only stored in a subset of the structural grids on the airfoil outer skin. The reference line is at the ¼-chord line. Five degrees of freedom are used in the 1-D model, including extension, twist, bending in two directions, and camber bending. The latter is defined by the finite-section mode of Fig. 2, given by

$$\psi_q(x_2,x_3) = \left[0, 0, r + s\left(\frac{2x_2}{c}\right) + \left(\frac{2x_2}{c}\right)^2\right] \tag{8}$$

where x_2 is the oblique chordwise coordinate referred to the mid-chord. r and s are included to remove the plunge and pitch components of the mode and are computed numerically. For the static aeroelastic analysis, a convergence criterion is defined in the two-norm of Z. Figure 3 shows the change in the Mach contours between the rigid and deformed wing for $t = 1\,\text{mm}$,

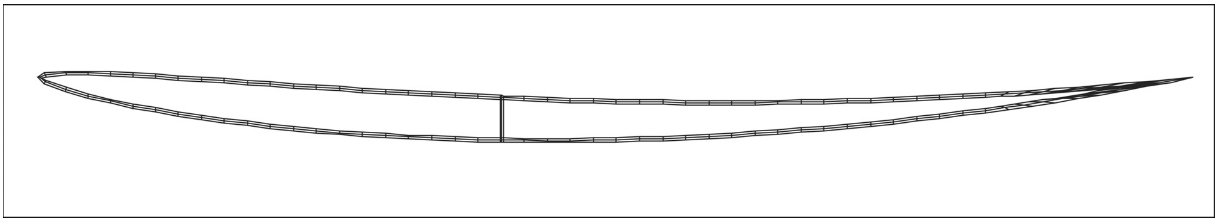

Fig. 2. Finite-section mode for camber-bending deformation.

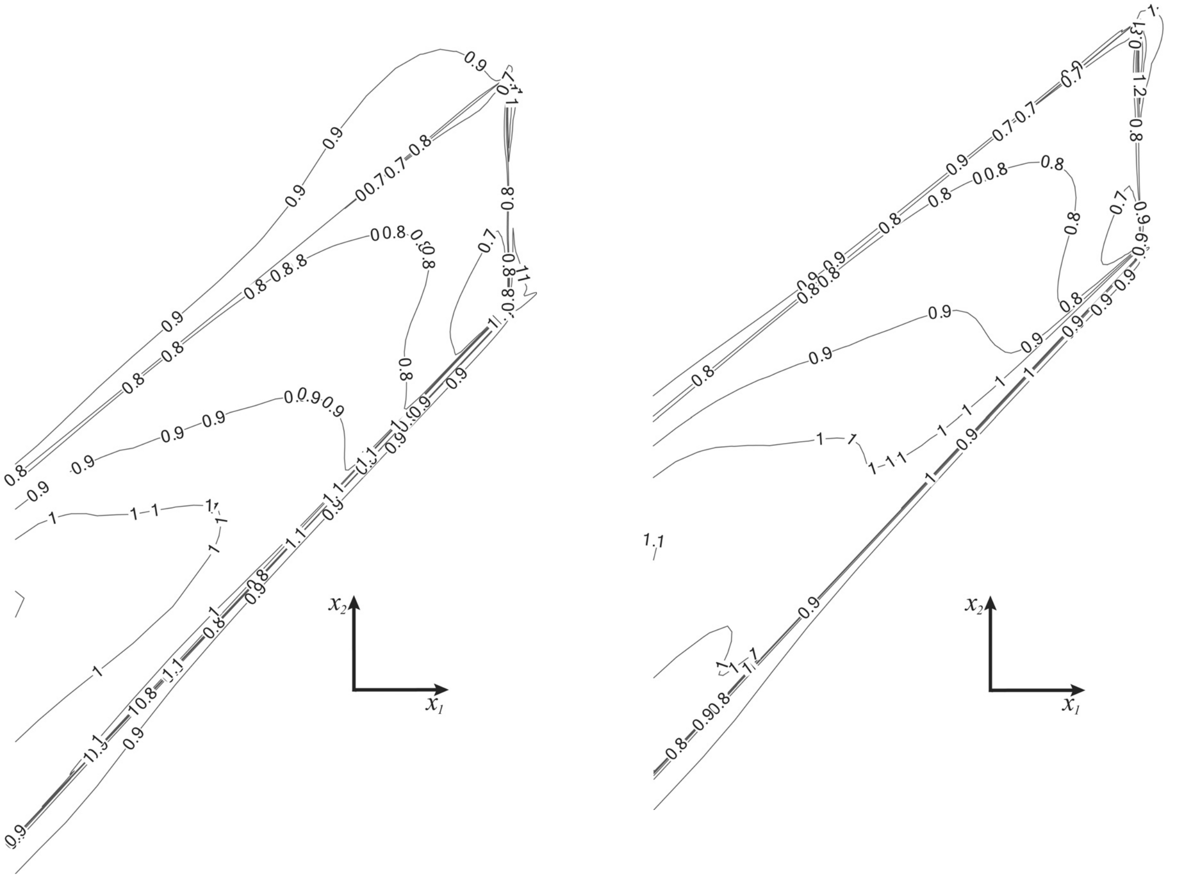

Fig. 3. Rigid (left) and static aeroelastic (right, $t = 1$ mm) distributions of Mach number on the upper wing at $M_\infty = 0.96$, $\alpha = 2°$.

$M_\infty = 0.96$, and $\alpha = 2°$. For this case, tip deflection is $0.052b$, tip pitch $0.33°$, and maximum amplitude of camber bending is $q_{max} = 1.4 \times 10^{-4}b$ (at 55% of span). The spanwise distribution of force coefficients for varying thickness is shown in Fig. 4, with coefficients defined as:

$$C_F = \frac{F}{\frac{1}{2}\rho V^2 c_r}, C_M = \frac{M}{\frac{1}{2}\rho V^2 c_r^2}, C_{F_q} = \frac{F_q}{\frac{1}{2}\rho V^2 c_r} \tag{9}$$

4. Conclusions

A new methodology for the aeroelastic analysis of highly-flexible slender wings has been introduced. It is based on an asymptotic decomposition of the 3-D elastic problem that provides an accurate representation of the deformation field in the case of large global displacements and rotations. Although the model is based on the reduction to the dynamics along a reference line, an arbitrary definition of the 1-D state variables is included to account for any possible deformation. As an example, the static aeroelastic characteristics of a wing based on

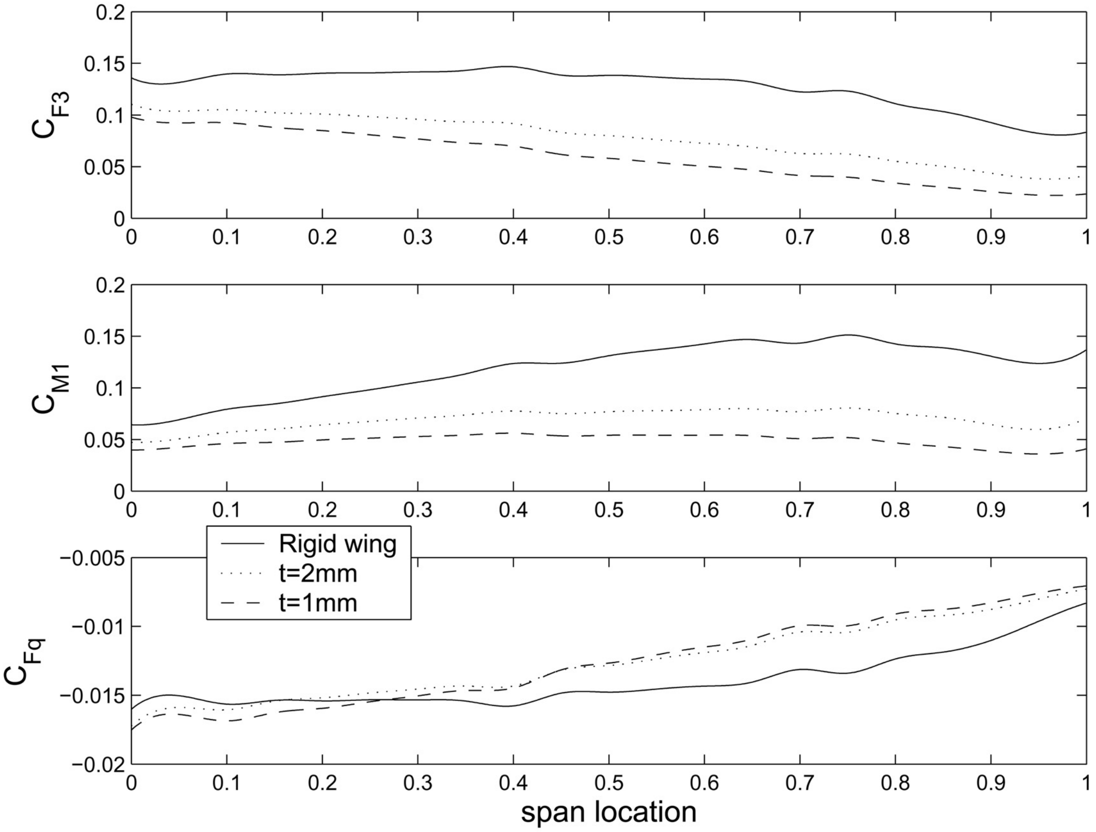

Fig. 4. Spanwise variation of lift and moment for varying flexibility ($M_\infty = 0.96$, $\alpha = 2°$).

the AGARD445.6 were studied using a five degrees-of-freedom model that included camber-bending deformation.

Acknowledgment

NASA Langley Research Center grant NAG-1-03038 monitored by Dr. David Schuster.

References

[1] Cesnik CES, Hodges DH. VABS: a new concept for composite rotor blade cross-sectional modeling. J American Helicopter Soc 1997;42:27–38.

[2] Palacios R, Cesnik CES. Cross-sectional analysis of non-homogeneous anisotropic active slender structures (to appear). AIAA Journal 2005.

[3] Smith MJ, Schuster DM, Huttsell L, Buxton B. Development of an Euler/Navier-Stokes aeroelastic method for three-dimensional vehicles with multiple flexible surfaces. AIAA Paper 1996–1513, 1996.

[4] Kingsley G, Siegel JM, Harrand VJ, Lawrence CL, Luker JJ. Development of a multi-disciplinary computing environment (MDICE). AIAA Paper 1998–4738, 1998.

[5] Yates EC, Jr. AGARD standard aeroelastic configuration for dynamic response, candidate configuration I: wing 445.6. NASA TM-100492, 1987.